J. Phys. Chem. A **2008,** *112,* 152−159

Addition Reaction of Adamantylideneadamantane with Br_2 and $2Br_2$: A Computational Study

Shahidul M. Islam and Raymond A. Poirier*

Department of Chemistry, Memorial University, St. John's, Newfoundland, Canada A1B 3X7

Received: September 11, 2007; In Final Form: October 16, 2007

Ab initio calculations were carried out for the reaction of adamantylideneadamantane (Ad=Ad) with Br_2 and $2Br_2$. Geometries of the reactants, transition states, intermediates, and products were optimized at HF and B3LYP levels of theory using the 6-31G(d) basis set. Energies were also obtained using single point calculations at the MP2/6-31G(d)//HF/6-31G(d), MP2/6-31G(d)//B3LYP/6-31G(d), and B3LYP/6-31+G(d)//B3LYP/6-31G(d) levels of theory. Intrinsic reaction coordinate (IRC) calculations were performed to characterize the transition states on the potential energy surface. Only one pathway was found for the reaction of Ad=Ad with one Br_2 producing a bromonium/bromide ion pair. Three mechanisms for the reaction of Ad=Ad with $2Br_2$ were found, leading to three different structural forms of the bromonium/Br_3^- ion pair. Activation energies, free energies, and enthalpies of activation along with the relative stability of products for each reaction pathway were calculated. The reaction of Ad=Ad with $2Br_2$ was strongly favored over the reaction with only one Br_2. According to B3LYP/6-31G(d) and single point calculations at MP2, the most stable bromonium/Br_3^- ion pair would form spontaneously. The most stable of the three bromonium/Br_3^- ion pairs has a structure very similar to the observed X-ray structure. Free energies of activation and relative stabilities of reactants and products in CCl_4 and CH_2ClCH_2Cl were also calculated with PCM using the united atom (UA0) cavity model and, in general, results similar to the gas phase were obtained. An optimized structure for the *trans*-1,2-dibromo product was also found at all levels of theory both in gas phase and in solution, but no transition state leading to the *trans*-1,2-dibromo product was obtained.

1. Introduction

Bromination of alkenes is a well-known organic reaction.[1,2] Experimentally, the reaction mechanism is considered to have several steps, depending on the alkene and solvent used.[2−7] A bromine/alkene charge-transfer complex (CTC) and the bromonium ion have been considered to be the main intermediates in the bromination of alkenes. The existence of a cyclic bromonium ion intermediate was first proposed by Roberts and Kimball.[8] However, no structural evidence of the occurrence of a cyclic bromonium ion was reported despite the many experimental attempts by a variety of techniques.[9−15] Strating and co-workers[16] first produced a bromonium ion tribromide in the lab by reacting adamantylideneadamantane (**1**) with Br_2 in $CC1_4$. Slebocka-Tilk et al.[17] for the first time obtained the X-ray structure of the adamantylideneadamantane bromonium ion with a Br_3^- counterion (**2**) (Scheme 1). Later, Brown et al.[18] also reported the existence of another bromonium ion of bicyclo [3.3.1]nonylidenebicyclo [3.3.l]nonane. (*E*)-2,2,5,5-tetramethyl-3,4-diphenylhex-3-ene (**3**) is the first reported example of an olefin whose interaction with bromine is limited to π complex formation (Scheme 2).[19] Similarly, tetraneopentylethylene (**4**) does not react with bromine in CCl_4 solution, and no π complex was formed between these two reagents on the basis of the ^{13}C NMR spectrum (Scheme 3).[20] Thus, the reactivity of olefins toward bromine depends on their steric hindrance.

Theoretical studies of the bromimination of alkenes are quite limited as compared to experiment. Yamabe et al.[21] studied the mechanism for the reactions $X_2 + C_2H_4 \rightarrow C_2H_4X_2$ [X = F, C1, and Br] at the MP3/3-21G//RHF/3-21G level of theory and found that the fluorination of ethene occurs via a four-centered transition state with an activation energy of 212.5 kJ mol^{-1}, while chlorination and bromination give a zwitterionic three-centered transition state with activation barriers of 212.1 and 256.9 kJ mol^{-1}, respectively. Hamilton and Schaefer[22] in their study on the structure and energetics of $C_2H_4Br^+$ isomers also proposed that the transition state is a three-membered bromonium ion with a nearby counter bromide ion. Recently, Cammi et al.[23] studied the bromination of ethene but only from the CTC to the transition state (TS) at the MP2/CEP-121G(aug) level of theory. The free energy barrier in going from the CTC to the TS was found to be 250.8 kJ mol^{-1} in the gas phase and 34.2 kJ mol^{-1} in water.

Recently,[24] we investigated the bromination reaction for a series of simple alkenes, namely, ethene, propene, isobutene, flouroethene, chloroethene, (*E*)-1,2-difluoroethene, and (*E*)-1,2-dichloroethene. It was found that Br_2 can react with alkenes via two different mechanisms. One involves a perpendicular attack by Br_2 to the C=C bond by a one-step pathway producing the bromonium/bromide ion pair intermediate. The second mechanism consists of a sidewise attack by Br_2 to the C=C bond, producing first the bromonium/bromide ion pair intermediate, which then produces the *trans*-1,2-dibromoalkane via multiple steps. Ethene can react with $2Br_2$ via several mechanisms, all leading to the *trans*-1,2-dibromoethane product. It was found that in this case, the bromination reaction in gas phase and in nonpolar aprotic solvents was mediated by the second bromine molecule. The most likely pathway for the reaction of

---

* Corresponding author. Tel.: (709) 737-8609; fax: (709) 737-3702; e-mail: rpoirier@mun.ca.

10.1021/jp077306d CCC: $40.75

SCHEME 1

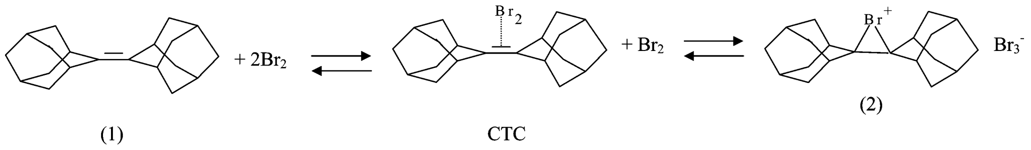

SCHEME 2

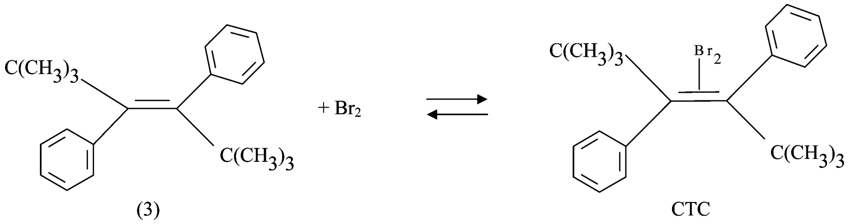

SCHEME 3

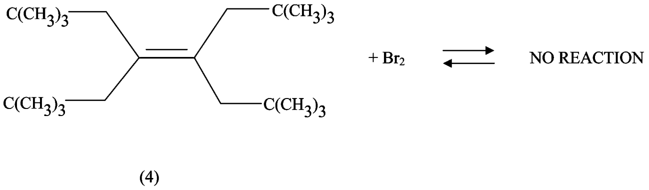

ethene and $2Br_2$ was found to be a multiple-step process involving the formation of an ethane bromonium/Br_3^- ion pair intermediate, which then leads to the formation of the 1,2-dibromo product by trans addition of a Br atom from Br_3^- to one of the bromonium ion carbons. The corresponding activation energy was 122.7 kJ mol^{-1} at the G3MP2B3 level of theory. For nonpolar aprotic solvents such as CH_2Cl_2 and CH_2ClCH_2Cl, the overall activation energies for the ethene + $2Br_2$ reaction were found to be 64.6 and 52.7 kJ mol^{-1}, respectively, at the B3LYP/6-31G(d) level of theory. This is in excellent agreement with the experimental activation energy of 66.4 kJ mol^{-1} for the reaction in CCl_2H-CCl_2H.[25] However, in polar protic solvents such as CH_3OH, the calculated free energy agreed very well with experiment[26] only when the reaction was mediated by a single CH_3OH molecule. A kinetic expression was proposed that accounts for the difference between bromination of alkenes in protic and non-protic solvents.

In this study, we investigated the mechanism for the reaction of bromine with adamantylideneadamantane, which is known to stop the reaction by producing a bromonium/tribromide ion pair.[16,17] The typical bridged bromonium ion would be in this case Ad=Ad sterically hindered by four conformationally constrained axial hydrogen atoms of the cyclohexane moiety as illustrated in Figure 1. Therefore, no further reaction occurred to form the dibromo product. No reaction can occur even with small nucleophiles such as fluoride ions.[27] Although the reaction mechanism of Ad=Ad with Br_2 was extensively studied previously,[3,16,17,27−31] no computational study was conducted to investigate the mechanism of the bromination of Ad=Ad. A potential energy surface for the bromination reaction of Ad=Ad that leads to the bromonium/tribromide ion pair will provide further insight into the bromination reaction of alkenes. It is difficult to extract conclusive information about the mechanistic pathways from experiments only. Thus, quantum chemical calculations provide the only source for a detailed characterization of the potential energy surface along the reaction path.

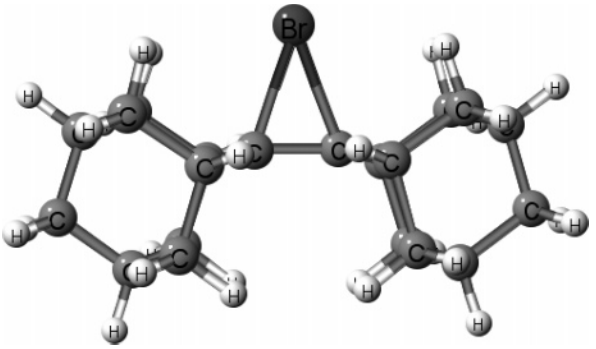

Figure 1. Expected structure of the adamantylideneadamantane bromonium ion.

2. Computational Method

All the electronic structure calculations were carried out with Gaussian 03.[32] The geometries of reactants, transition states, intermediates, and products were fully optimized at the HF and B3LYP levels of theory using the 6-31G(d) basis set. Energies were also obtained using MP2/6-31G(d)//HF/6-31G(d), MP2/6-31G(d)//B3LYP/6-31G(d), and B3LYP/6-31+G(d)//B3LYP/6-31G(d) single point calculations. Frequencies were calculated for all structures to ensure the absence of imaginary frequencies in the minima and for the presence of only one imaginary frequency in the transition states. The complete reaction pathways for all the mechanisms discussed in this study were verified using IRC analysis for all transition states. Structures at the last IRC points were optimized to positively identify the reactants and products to which each transition state is connected. Free energies of activation and relative stabilities of reactants and products in CCl_4 and CH_2ClCH_2Cl for the addition reaction of bromine to Ad=Ad were calculated with the polarizable continuum model (PCM) as implemented in Gaussian 03. All free energy calculations involving solvation were performed using the solution-phase structures optimized at the HF/6-31G(d) and B3LYP/6-31G(d) levels of theory. By default, the PCM model builds up the cavity using the united atom (UA0) model.

3. Results and Discussion

The results for the reaction of adamantylideneadamantane (Ad=Ad) with Br_2 and $2Br_2$ in the gas phase and in CCl_4 are given in Tables 1−5.

3.1. Potential Energy Surface for Reaction of Ad=Ad + Br_2: Pathway A. Pathway A is the only pathway found for the reaction of Ad=Ad with one Br_2. The structures involved in pathway A are shown in Figure 2. The relative energies of reactants, intermediates, transition states, and products are shown

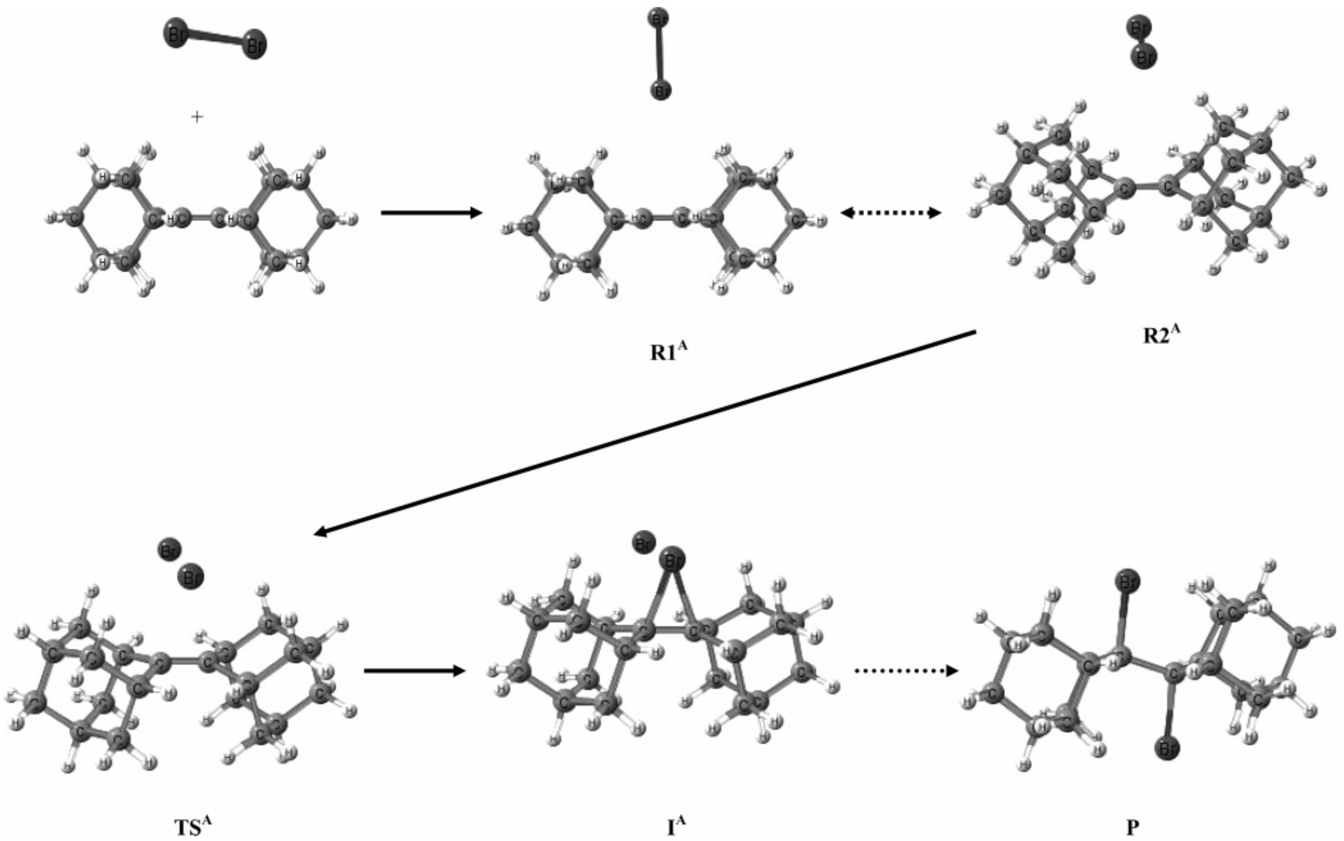

Figure 2. Mechanism for the reaction of Ad═Ad + Br_2 (pathway A).

TABLE 1: Activation Energies, Free Energies, and Enthalpies of Activation (kJ mol^{-1}) at 298.15 K for Reaction of Adamantalydineadamantane with Br_2 (Pathway A)[a]

level/basis set	$\Delta E_{a,TS}{}^A$	$\Delta H^{\ddagger}{}_{TS}{}^A$	$\Delta G^{\ddagger}{}_{TS}{}^A$
HF/6-31G(d)			
gas phase	272.8	269.4	281.8
CCl_4[b]			251.7
CH_2ClCH_2Cl[b]			234.8
MP2/6-31G(d)//HF/6-31G(d)			
gas phase	111.4		
B3LYP/6-31G(d)			
gas phase	134.7	131.0	141.4
CCl_4[b]			115.4
CH_2ClCH_2Cl[b]			97.5
MP2/6-31G(d)//B3LYP/6-31G(d)	145.3		
B3LYP/6-31+G(d)//B3LYP/6-31G(d)	106.0		

[a] Barriers were calculated from the Ad═Ad/Br_2 complex as defined in Figures 2 and 3. [b] PCM-United Atom model was used for optimized structures. In all cases, $\Delta G = \Delta\Delta G$ (thermal correction) + ΔG_{solv}.

in Figure 3. Activation energies, free energies, and enthalpies of activation for the reaction of Ad═Ad with Br_2 are given in Table 1. Ad═Ad can form two complexes with Br_2. In one complex, $R1^A$, Br_2 is coplanar and perpendicular to the C═C bond, and in the other complex, $R2^A$, Br−Br and C═C bonds are skewed to each other (Figure 2). All the levels except for HF predict $R1^A$ to be more stable than $R2^A$, by 21.2 kJ mol^{-1} at the B3LYP/6-31G(d) level of theory. Pathway A is a one-step mechanism in which the adamantylideneadamantane bromonium/Br^- ion pair (I^A) is formed via transition state TS^A, where one Br attacks the C═C bond of Ad═Ad. In the reactant complex $R2^A$, the Br−Br and C═C bond distances are 2.316 and 1.349 Å, respectively, at the B3LYP/6-31G(d) level of theory, while in TS^A, the distances increase to 3.058 and 1.419 Å, respectively. On the other hand, the Br−C bond distance in $R2^A$ decreases from 4.719 to 2.751 Å in TS^A. IRC analysis confirmed that TS^A leads to $R2^A$ and I^A. The activation energy ($\Delta E_{a,TS}{}^A$) for the reaction of Ad═Ad with Br_2 is 272.8 and 134.7 kJ mol^{-1} at the HF/6-31G(d) and B3LYP/6-31G(d) levels of theory, respectively. At MP2/6-31G(d)//HF/6-31G(d), the barrier is lowered to 111.4 kJ mol^{-1}, while at MP2/6-31G(d)//B3LYP/6-31G(d), the barrier is increased to 145.3 kJ mol^{-1}. The surprising lowering in the barrier by 161.4 kJ mol^{-1} at MP2/6-31G(d)//HF/6-31G(d) suggests both the importance of electron correlation and different PES at MP2 and HF. The B3LYP/6-31+G(d)//B3LYP/6-31G(d) calculation decreases the B3LYP/6-31G(d) barrier by 28.7 to 106.0 kJ mol^{-1}. The solvent model used in this study predicts a free energy of activation of 251.7 and 115.4 kJ mol^{-1} in CCl_4 and 234.8 and 97.5 kJ mol^{-1} in

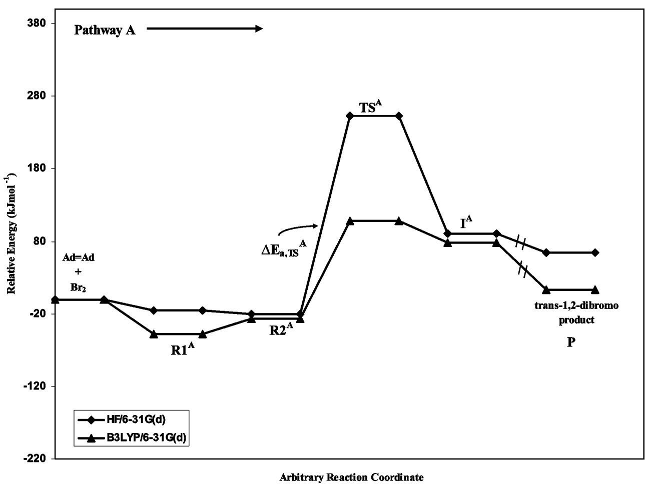

Figure 3. Reaction pathway for the reaction of Ad═Ad + Br_2 (pathway A) at HF/6-31G(d) and B3LYP/6-31G(d) levels of theory (see Figure 2 for structures).

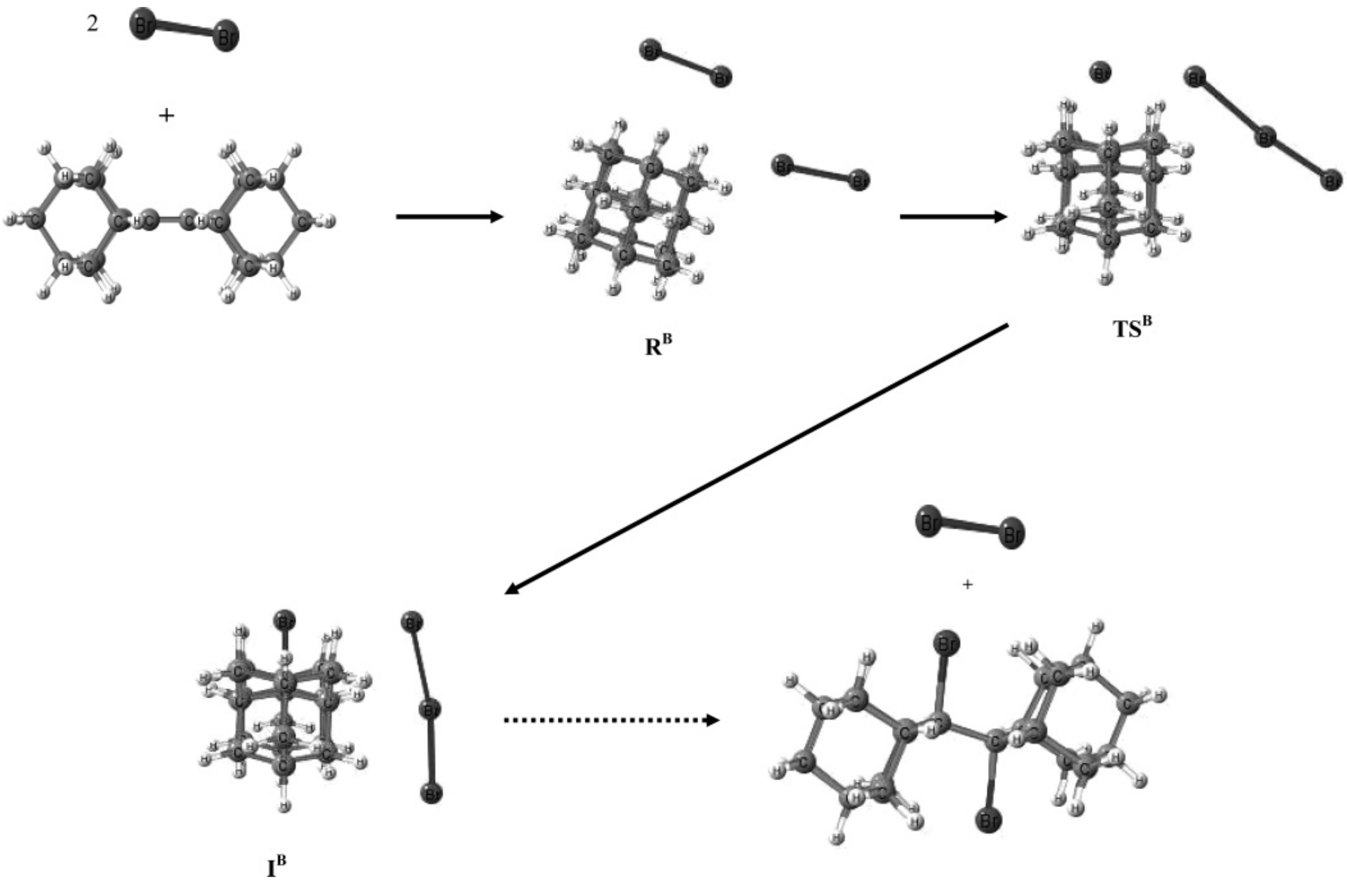

Figure 4. Mechanism for the reaction of Ad═Ad + $2Br_2$ (pathway B).

CH_2ClCH_2Cl at HF/6-31G(d) and B3LYP/6-31G(d), respectively. Although optimized structures for the *trans*-1,2-dibromo product (P) were obtained by all levels of theory, no transition state leading from I^A to P was obtained despite successive attempts. P was found to be more stable than I^A by 26.4 and 64.2 kJ mol^{-1} at the HF/6-31G(d) and B3LYP/6-31G(d) levels of theory, respectively. It is interesting to note that no optimized structure for the *cis*-1,2-dibromo product was found in this study despite successive attempts by different levels of theory.

3.2. Potential Energy Surfaces for the Reaction of Ad═Ad with $2Br_2$. The results for the reaction of Ad═Ad and $2Br_2$ will be discussed in the following order: (1) pathway B, (2) pathway C, and (3) pathway D.

3.2.1. Pathway B. The structures involving pathway B are shown in Figure 4. The relative energies of reactants, intermediates, and transitions states are shown in Figure 5. Activation energies, free energies, and enthalpies of activation for pathway B are given in Table 2. Reactant complex (R^B) of Ad═Ad + $2Br_2$ is similar to $R2^A$, except that the second Br_2 interacts sidewise. Pathway B is a one-step mechanism in which an ion pair of the bromonium ion and Br_3^- ion is formed via a transition state TS^B where one Br atom of Br_2 attacks the C═C bond of Ad═Ad, while the other Br atom transfers to the other Br_2. In the reactant complex R^B, the Br−Br bond distance for Br_2 attacking the C═C bond is 2.329 Å at the B3LYP/6-31G(d) level of theory, while in TS^B, the distance increases to 2.878 Å. The C−Br (Br attacking the C═C) and Br···Br_2 bond distances start at 4.699 and 3.172 Å in R^B and decrease to 2.904 and 2.723 Å in TS^B, respectively, at B3LYP/6-31G(d). IRC analysis confirmed that TS^B leads to R^B and I^B. The activation energy for the reaction of Ad═Ad with $2Br_2$ in pathway B is 256.8 kJ mol^{-1} at HF/6-31G(d) and 94.1 kJ mol^{-1} at B3LYP/6-31G(d). The activation energies at MP2/6-31G(d)//HF/6-31G(d) and MP2/6-31G(d)//B3LYP/6-31G(d) are 91.6 and 91.8 kJ mol^{-1}, respectively, in excellent agreement with the B3LYP/6-31G(d) results. The barrier decreases to 64.4 kJ mol^{-1} at the B3LYP/6-31+G(d)//B3LYP/6-31G(d) level of theory. Applying the solvent model yields a mechanism very similar to the gas phase one. The solvent model used in this study predicts that the free energy of activation for this reaction would be lowered in CCl_4 and CH_2ClCH_2Cl by 15.1 and 26.8 kJ mol^{-1}, respectively, at B3LYP/6-31G(d).

3.2.2. Pathway C. The structures of reactants, intermediates, transitions states, and products of pathway C are shown in Figure 6 for the reaction of Ad═Ad and $2Br_2$. The relative energies of

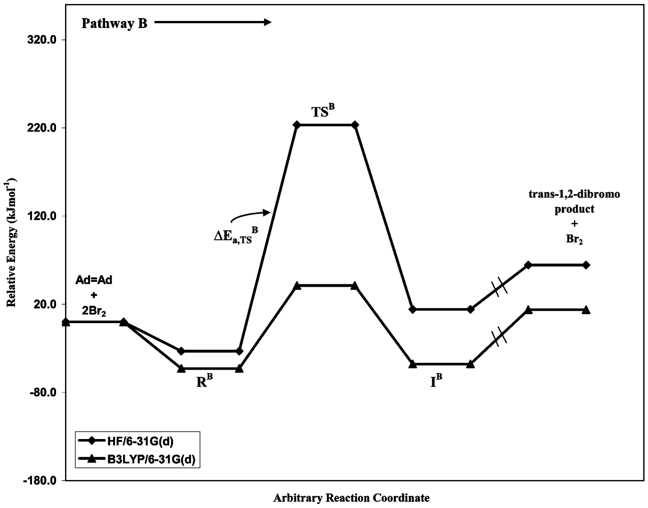

Figure 5. Reaction pathway for the reaction of Ad═Ad + $2Br_2$ (pathway B) at HF/6-31G(d) and B3LYP/6-31G(d) levels of theory (see Figure 4 for structures).

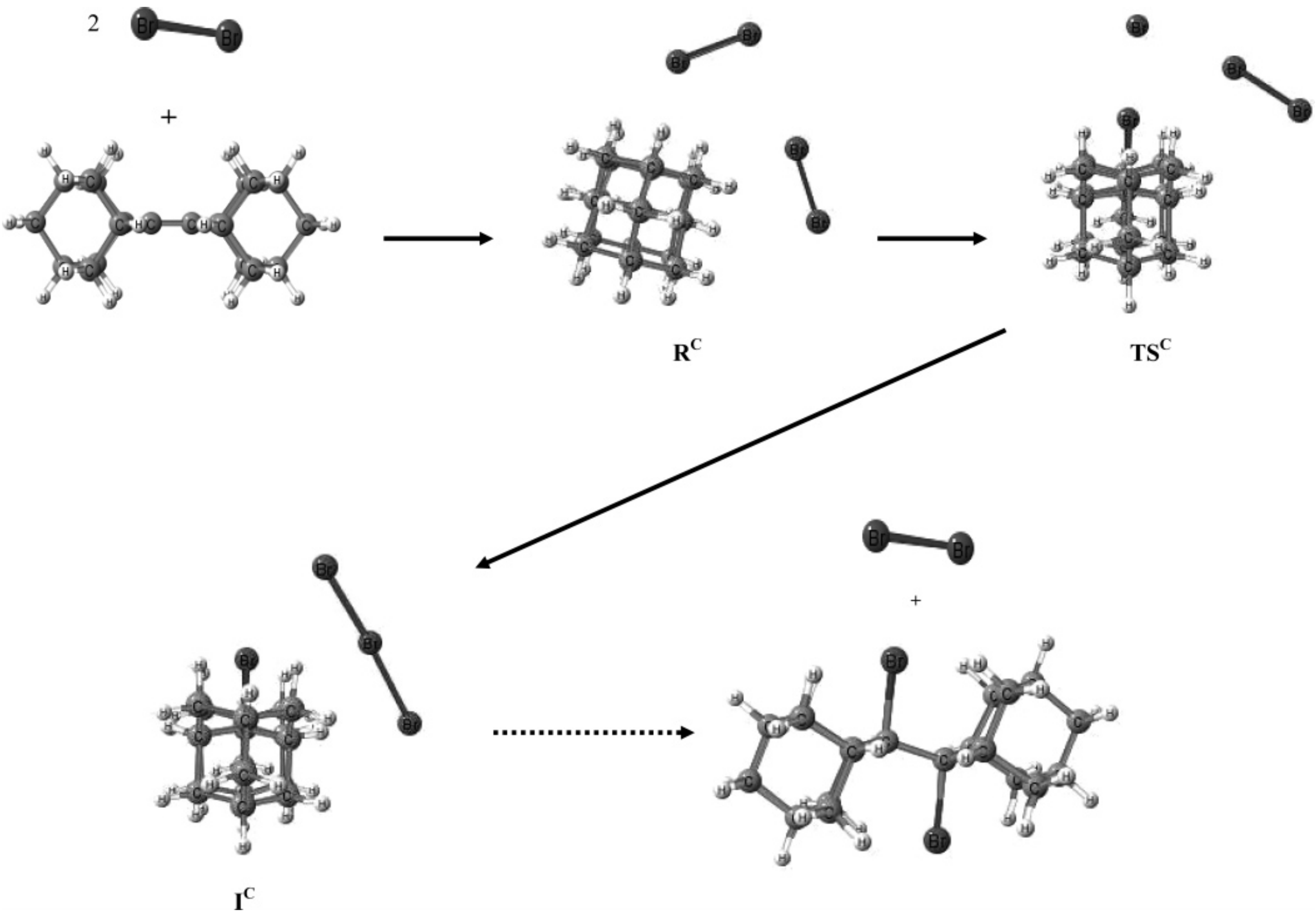

Figure 6. Mechanism for the reaction of Ad═Ad + $2Br_2$ (pathway C).

TABLE 2: Activation Energies, Free Energies, and Enthalpies of Activation (kJ mol^{-1}) at 298.15 K for Reaction of Adamantalydineadamantane with $2Br_2$ (Pathway B)[a]

level/basis set	$\Delta E_{a,TS}{}^{B}$	$\Delta H^{\ddagger}{}_{TS}{}^{B}$	$\Delta G^{\ddagger}{}_{TS}{}^{B}$
HF/6-31G(d)			
gas phase	256.8	255.7	263.1
CCl_4[b]			240.8
CH_2ClCH_2Cl[b]			217.4
MP2/6-31G(d)//HF/6-31G(d)			
gas phase	91.6		
B3LYP/6-31G(d)			
gas phase	94.1	90.0	97.5
CCl_4[b]			82.4
CH_2ClCH_2Cl[b]			70.7
MP2/6-31G(d)//B3LYP/6-31G(d)	91.8		
B3LYP/6-31+G(d)//B3LYP/6-31G(d)	64.4		

[a] Barriers were calculated from the Ad═Ad/$2Br_2$ complex as defined in Figures 4 and 5. [b] PCM−United Atom model was used for optimized structures. In all cases, $\Delta G = \Delta\Delta G$ (thermal correction) + ΔG_{solv}.

reactants, intermediates, transitions states, and products are shown in Figure 7. Activation energies, free energies, and enthalpies of activation for pathway C are given in Table 3.

In pathway C, intermediate I^C is formed via TS^C, which differs from TS^B in that the Br_2 attacking the C═C bond of Ad═Ad is tilted from the perpendicular. This leads to a different bromonium/Br_3^- ion pair (I^C). In the reactant complex R^C, the Br−Br bond distance of Br_2 that attacks the C═C is 2.284 Å at the HF/6-31G(d) level of theory, while in TS^C, the same Br−Br distance increases to 2.748 Å. The corresponding activation energy ($\Delta E_{a.TS}{}^{C}$) is 61.3 kJ mol^{-1} at HF/6-31G(d). No transition state structure was found at the B3LYP/6-31G(d) level of theory; however, both R^C and I^C were obtained at this level. The MP2/6-31G(d)//HF/6-31G(d) and B3LYP/6-31G(d)// HF/6-31G(d) single point calculations predict a negative barrier (Table 3 and Figure 7). The B3LYP results therefore suggest that the reaction would be barrierless and occur spontaneously in the gas phase. This pathway was only found in the gas phase. Optimization of TS^C in solution leads to a slightly different transition state, which corresponds to a different pathway, pathway D. Since R^B and R^C differ by only 3.1 kJ mol^{-1} at B3LYP/6-31G(d), a simple $R^B \rightarrow R^C$ conversion is more likely to occur.

3.2.3. Pathway D. The structures involved in pathway D are shown in Figure 8. The relative energies of reactants, intermedi-

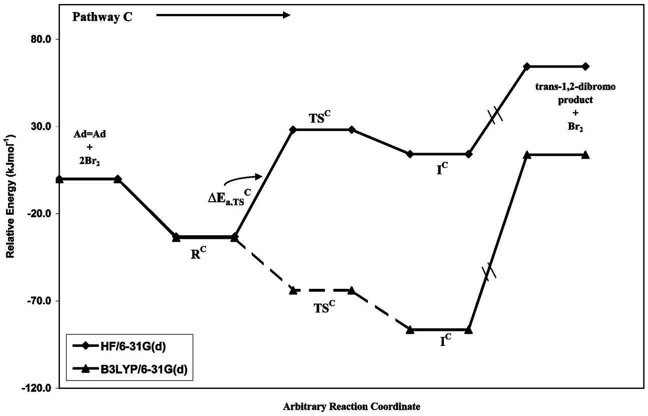

Figure 7. Reaction pathway for the reaction of Ad═Ad + $2Br_2$ (pathway C) at HF/6-31G(d) level of theory. For R^C and TS^C, B3LYP/6-31G(d)//HF/6-31G(d) single point energies are indicated by dashed lines (see Figure 6 for structures).

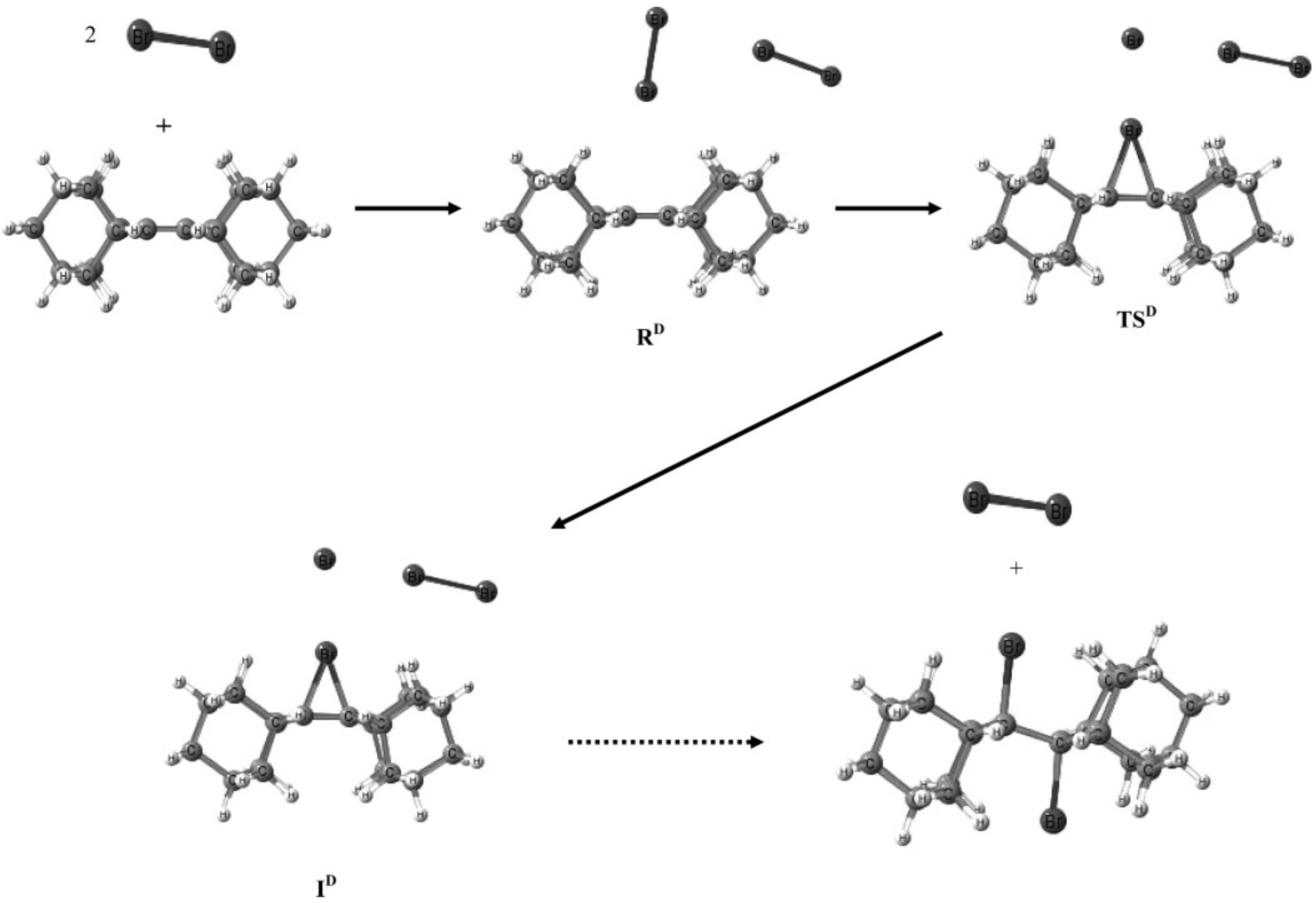

Figure 8. Mechanism for the reaction of Ad═Ad + $2Br_2$ (pathway D).

TABLE 3: Activation Energies, Free Energies, and Enthalpies of Activation (kJ mol^{-1}) at 298.15 K for Reaction of Adamantalydineadamantane with $2Br_2$ (Pathway C) in the Gas Phase[a]

level/basis set	$\Delta E_{a,TS^C}$	$\Delta H^{\ddagger}_{TS^C}$	$\Delta G^{\ddagger}_{TS^C}$
HF/6-31G(d)	61.3	60.5	80.2
MP2/6-31G(d)//HF/6-31G(d)	−46.0		
B3LYP/6-31G(d)//HF/6-31G(d)	−30.2		
B3LYP/6-31+G(d)//HF/6-31G(d)	−44.7		

[a] Barriers were calculated from the Ad═Ad/$2Br_2$ complex as defined in Figures 6 and 7.

ates, and transitions states are shown in Figure 9. Activation energies, free energies, and enthalpies of activation for pathway D are given in Table 4.

In addition to the two bromonium/Br_3^- ion pairs (I^B and I^C), a third bromonium/Br_3^- ion pair (I^D) is formed via TS^D in pathway D, with an activation energy ($\Delta E_{a.TS^D}$) of only 54.8 kJ mol^{-1} at HF/6-31G(d). The structure of TS^D involves a perpendicular attack by a Br_2 on the C═C bond, while the other Br_2 is coplanar with the C═C bond and the attacking Br_2. In the reactant complex R^D, the Br_2 that attacks the C═C has a Br−Br bond distance of 2.285 Å at HF/6-31G(d), while in TS^D, it increases to 2.805 Å. This bromonium/Br_3^- ion pair (I^D) is very similar to that observed experimentally.[17] No reactant complex (R^D) or transition state (TS^D) was found at the B3LYP/6-31G(d) level of theory. The MP2/6-31G(d)//HF/6-31G(d) and B3LYP/6-31G(d)//HF/6-31G(d) single point calculations predict, as for pathway C, that the reaction is barrierless in the gas phase. This mechanism is also observed in CCl_4 and CH_2ClCH_2Cl. The free energies of activation in CCl_4 and CH_2ClCH_2Cl decrease by 45.1 and 74.5 kJ mol^{-1} at HF/6-31G(d), suggesting that the reaction is most likely barrierless in solution as well. This is in accordance with experiment,[31] where an equilibrium mixture of Ad═Ad + $2Br_2$ $\rightleftarrows$ adamantylideneadamantane bromonium/Br_3^- was reported with no evidence of any Ad═Ad/$2Br_2$ complex formation. Furthermore, the reaction is also highly favored with $\Delta E = -135.7$ kJ mol^{-1} at B3LYP/6-31+G(d)//B3LYP/6-31G(d) and -144.1 kJ mol^{-1} at MP2/6-31G(d)//B3LYP/6-31G(d).

3.3. Relative Stabilities. The relative energies of the *trans*-1,2-dibromo product (P), bromonium/Br^- ion pair (I^A), and three bromonium/Br_3^- ion pairs (I^B, I^C, and I^D) are given in Table 5. All the levels of theory predict P to be more stable than I^A with

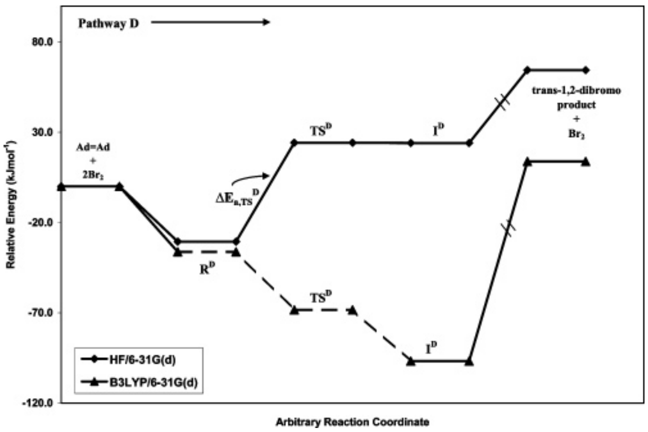

Figure 9. Reaction pathway for the reaction of Ad═Ad + $2Br_2$ (pathway D) at HF/6-31G(d) level of theory. For R^D and TS^D, B3LYP/6-31G(d)//HF/6-31G(d) single point energies are indicated by dashed lines (see Figure 8 for structures).

TABLE 4: Activation Energies, Free Energies, and Enthalpies of Activation (kJ mol^{-1}) at 298.15 K for Reaction of Adamantalydineadamantane with 2Br$_2$ (Pathway D)[a]

level/basis set	$\Delta E_{a,TS}{}^{D}$	$\Delta H^{\ddagger}{}_{TS}{}^{D}$	$\Delta G^{\ddagger}{}_{TS}{}^{D}$
HF/6-31G(d)			
gas phase	54.8	54.2	81.3
CCl$_4$[b]			36.2
CH$_2$ClCH$_2$Cl[b]			6.8[c]
MP2/6-31G(d)//HF/6-31G(d)	−52.3		
B3LYP/6-31G(d)//HF/6-31G(d)	−32.2		
B3LYP/6-31+G(d)//HF/6-31G(d)	−55.6		

[a] Barriers were calculated from the Ad═Ad/2Br$_2$ complex as defined in Figures 8 and 9, respectively. [b] PCM−United Atom model was used for optimized structures. In all cases, $\Delta G = \Delta\Delta G$ (thermal correction) + ΔG_{solv}. [c] Single-point calculation using the HF/6-31G(d) optimized gas-phase structure.

$\Delta E = -26.4$ at HF/6-31G(d) and $\Delta E = -64.2$ kJ mol^{-1} at B3LYP/6-31G(d). There is excellent agreement between the MP2/6-31G(d)//HF/6-31G(d) and the MP2/6-31G(d)//B3LYP/6-31G(d) values of −93.2 and −90.8 kJ mol^{-1}, respectively, which are in reasonable agreement with the B3LYP/6-31G(d) value of −64.2 kJ mol^{-1}. All the levels of theory also predict ΔG ($I^A \rightarrow P$) to be negative in the gas phase (Table 5). However, in CH$_2$ClCH$_2$Cl, ΔG ($I^A \rightarrow P$) becomes positive with values of 102.4 and 38.4 kJ mol^{-1} at HF/6-31G(d) and B3LYP/6-31G(d), respectively. Therefore, the bromonium/Br$^-$ (I^A) is favored over the 1,2-dibromo product (P) in CH$_2$ClCH$_2$Cl. In CCl$_4$, according to HF/6-31G(d), I^A is favored ($\Delta G = 40.4$ kJ mol^{-1}), while according to the B3LYP/6-31G(d) level of theory, the dibromo product (P) is slightly favored ($\Delta G = -12.7$ kJ mol^{-1}).

Comparing the three bromonium/Br$_3{}^-$ ion pairs (I^B, I^C, and I^D), I^D is predicted (except HF) to be the most stable in both gas phase and solution. I^D is more stable than I^B with ΔE ($I^B \rightarrow I^D$) of −49.1 kJ mol^{-1} at B3LYP/6-31G(d). Single point calculations at MP2/6-31G(d)//HF/6-31G(d) and MP2/6-31G(d)//B3LYP/6-31G(d) also predict I^D to be more stable than I^B by −15.2 and −41.8 kJ mol^{-1}, respectively. At the B3LYP/6-31G(d) level of theory, ΔG is −51.5 kJ mol^{-1}. I^D is also predicted to be more stable in CCl$_4$ and CH$_2$ClCH$_2$Cl solutions with ΔG values of −31.0 and −24.5 kJ mol^{-1}, respectively. For $I^C \rightarrow I^D$, I^C is found to be more stable than I^D at HF/6-31G(d) ($\Delta E = 9.8$ kJ mol^{-1}), and I^D is found to be more stable at B3LYP/6-31G(d) ($\Delta E = -10.4$ kJ mol^{-1}). ΔG ($I^C \rightarrow I^D$) is found to be negative with a value of −15.9 kJ mol^{-1} at B3LYP/6-31G(d) in the gas phase. All the levels of theory also predict ΔG to be negative in CCl$_4$ and in CH$_2$ClCH$_2$Cl with values of −0.2 and −4.6 kJ mol^{-1}, respectively, at HF/6-31G(d) and −10.2 and −8.2 kJ mol^{-1}, respectively, at B3LYP/6-31G(d). For $I^D \rightarrow$ *trans*-1,2-dibromo product (P) + Br$_2$, ΔE is 40.5 kJ mol^{-1} at HF/6-31G(d) and 110.6 kJ mol^{-1} at B3LYP/6-31G(d). All the levels of theory also predict ΔG ($I^D \rightarrow P + Br_2$) to be positive with ΔE values of 17.6 and 108.4 kJ mol^{-1} at HF/6-31G(d) and B3LYP/6-31G(d), respectively. This again suggests that I^D is a very stable structure. Similar results were also obtained in CCl$_4$ and CH$_2$ClCH$_2$Cl solution (Table 5). Therefore, bromination of adamantylideneadamantane will undoubtedly favor the formation of I^D in CCl$_4$ and CH$_2$ClCH$_2$Cl, which is in excellent agreement with the X-ray structure.[17] To investigate if I^D dissociates into the adamantylideneadamantane bromonium ion (Ad−Ad-Br$^+$) and Br$_3{}^-$, we tried to optimize the dissociated products. It is interesting to see that despite successive attempts with both HF and B3LYP levels of theory, an optimized structure for Ad−Ad-Br$^+$ (Figure 1) was not found in the gas phase or in solution (CCl$_4$ and CH$_2$ClCH$_2$Cl).

4. Conclusion

A comprehensive investigation was conducted to obtain all possible mechanisms involved in the reaction of Ad═Ad with Br$_2$ and 2Br$_2$. Only one pathway, pathway A, was found for the reaction of Ad═Ad with one Br$_2$ producing a bromonium/Br$^-$ ion pair (I^A). For the reaction of Ad═Ad with 2Br$_2$, three different pathways, pathways B−D, all producing bromonium/Br$_3{}^-$ ion pairs (I^B, I^C, and I^D), were found. Structures for pathways A and B were obtained at both HF and B3LYP levels of theory, while for pathways C and D, all structures were only obtained at the HF level. According to the HF/6-31G(d) level, both pathways C and D are the most favored pathways with very low activation energies as compared to pathways A and B (Tables 1−4). The HF/6-31G(d) activation energies were lowered by 138.1 and 162.7 kJ mol^{-1} at B3LYP/6-31G(d) for pathways A and B, respectively. Since the activation energy is significantly lower for the reaction of Ad═Ad with 2Br$_2$ as compared to the reaction with a single Br$_2$, the addition of bromine to Ad═Ad is indeed mediated by a second Br$_2$ molecule where the second Br$_2$ assists in the ionization of the reactant complex to form a bromonium/Br$_3{}^-$ ion pair. This is in agreement with our previous study on the bromination reaction of ethene.[24] According to B3LYP/6-31G(d), the reaction would occur spontaneously in the gas phase as well as in some solvents without a barrier to yield I^C and I^D via pathways C and D, respectively. Single point calculations at MP2/6-31G(d)//HF/6-31G(d) and MP2/6-31G(d)//B3LYP/6-31G(d) also

TABLE 5: Relative Stabilities (kJ mol^{-1}) at 298.15 K

	$I^A \rightarrow P$			$I^B \rightarrow I^D$			$I^C \rightarrow I^D$			$I^D \rightarrow P + Br_2$[a]		
level/basis set	ΔE	ΔH	ΔG	ΔE	ΔH	ΔG	ΔE	ΔH	ΔG	ΔE	ΔH	ΔG
HF/6-31G(d)												
gas phase	−26.4	−21.9	−9.9	2.1	2.7	2.0	9.8	10.2	7.6	40.5	40.2	17.6
CCl$_4$[b]			40.4			−3.1			−0.2			48.6
CH$_2$ClCH$_2$Cl[b]			102.4			−8.5			−4.6			93.8
MP2/6-31G(d)//HF/6-31G(d)												
gas phase	−93.2			−15.2			8.0			47.8		
B3LYP/6-31G(d)												
gas phase	−64.2	-59.8	−47.9	−49.1	−45.3	−51.5	−10.4	−7.4	−15.9	110.6	108.2	84.1
CCl$_4$[b]			−12.7			−31.0			−10.2			83.4
CH$_2$ClCH$_2$Cl[b]			38.4			−24.5			−8.2			108.4
MP2/6-31G(d)//B3LYP/6-31G(d)												
gas phase	90.8			−41.8			−6.0			80.5		

[a] Since the values are relatively large, we have neglected BSSE correction. [b] PCM−United Atom model was used for optimized structures. In all cases, $\Delta G = \Delta\Delta G$ (thermal correction) + ΔG_{solv}.

predict no barrier for pathways C and D. This is certainly worth investigating, and we hope that gas-phase experimentalists will test this prediction. No transition state leading from the bromonium/Br^- or bromonium/Br_3^- ion pair to the *trans*-1,2-dibromo product (P) was obtained for the pathways investigated despite successive attempts. The most stable bromonium/Br_3^- ion pair (I^D) corresponds to the observed X-ray structure.[17] I^D was also predicted to be the most stable structure in CCl_4 and CH_2ClCH_2Cl and would form spontaneously via pathway D.

Barriers and relative stabilities calculated using the MP2 level of theory were generally in better agreement with B3LYP than HF. Because of the size of the system, only optimization at HF/6-31G(d) and B3LYP/6-31G(d) and MP2/6-31G(d)//HF/6-31G(d), MP2/6-31G(d)//B3LYP/6-31G(d), and B3LYP/6-31+G(d)//HF/6-31G(d) single point calculations were possible. Our previous work on the bromination of alkenes[24] suggests that these are reliable levels of theory for this system.

Acknowledgment. We are grateful to the Natural Sciences and Engineering Council of Canada (NSERC) for financial support and the Atlantic Computational Excellence Network (ACEnet) for computer time.

Supporting Information Available: Full geometries and energies of all structures for reaction of Ad=Ad with Br_2 and $2Br_2$. This material is available free of charge via the Internet at http://pubs.acs.org.

References and Notes

(1) Smith, M. B.; March, J. *March's Advanced Organic Chemistry: Reactions, Mechanisms, and Structure*, 6th ed.; John Wiley and sons, Inc.: New York, 2007.

(2) Mare, P. B. D.; Bolton, R. *Electrophilic Additions to Unsaturated Systems*; Elsevier: Amsterdam, 1982.

(3) Brown, R. S.; Slebocka-Tilk, H.; Bennet, A. J.; Bellucci, G.; Bianchini, R.; Ambrosetti, R. *J. Am. Chem. Soc.* **1990**, *112*, 6310−6316.

(4) Schmid, G. H.; Garrat, D. G. Electrophilic additions to carbon-carbon double bonds. *The Chemistry of Double-Bonded Functional Groups*; Patai, S., Ed.; Wiley: New York, 1977; Suppl. A, Part 2, p 725.

(5) Brown, R. S.; Gedye, R.; Slebocka-Tilk, H.; Buschek, J.; Kopecky, K. *J. Am. Chem. Soc.* **1984**, *106*, 4515−4521.

(6) Bellucci, G.; Chiappe, C.; Marioni, F. *J. Am. Chem. Soc*. **1987**, *109*, 515−522.

(7) Bellucci, G.; Bianchini, R.; Chiappe, C.; Marioni, F.; Spagna, R. *J. Am. Chem. Soc.* **1988**, *110*, 546−552.

(8) Roberts, I.; Kimball, G. E. *J. Am. Chem. Soc*. **1937**, *59*, 947−948.

(9) Berman, D. W.; Anicich, V.; Beauchamp, J. L. *J. Am. Chem. Soc*. **1979**, *101*, 1239−1248.

(10) Wieting, R. D.; Staley, R. H.; Beauchamp, J. L. *J. Am. Chem. Soc*. **1974**, *96*, 7552−7554.

(11) Staley, R. H.; Wieting, R. D.; Beauchamp, J. L. *J. Am. Chem. Soc*. **1977**, *99*, 5964−5972.

(12) Kim, J. K.; Findlay, M. C.; Henderson, W. G.; Caserio, M. C. *J. Am. Chem. Soc*. **1973**, *95*, 2184−2193.

(13) Angelini, G.; Speranza, M. *J. Am. Chem. Soc*. **1981**, *103*, 3792−3799.

(14) Tsai, B. P.; Werner, A. S.; Baer, T. *J. Chem. Phys.* **1975**, *63*, 4384−4392.

(15) McLafferty, F. W. *Anal. Chem*. **1962**, *34*, 2−15.

(16) Strating, J.; Wieringa, J. H.; Wynberg, H. *J. Chem. Soc. D*. **1969**, 907−908.

(17) Slebocka-Tilk, H.; Ball, R. G.; Brown, R. S. *J. Am. Chem. Soc*. **1985**, *107*, 4504−4508.

(18) Brown, R. S.; Nagorski, R. W.; Bennet, A. J.; McClung, R. E. D.; Aarts, G. H. M.; Klobukowski, M.; McDonald, R.; Santarsiero, B. D. *J. Am. Chem. Soc*. **1994**, *116*, 2448−2456.

(19) Bellucci, G.; Chiappe, C.; Bianchini, R.; Lenoir, D.; Herges, R. *J. Am. Chem. Soc*. **1995**, *117*, 12001−12002.

(20) Olah, G. A.; Prakash, G. K. S. *J. Org. Chem*. **1977**, *42*, 580−582.

(21) Yamabe, S.; Minato, T.; Inagaki, S. *J. Chem. Soc., Chem. Commun*. **1988**, 532.

(22) Hamilton, T. P.; Schaefer, H. F. *J. Am. Chem. Soc*. **1990**, *112*, 8260−8265.

(23) Cammi, R.; Mennucci, B.; Pomelli, C.; Cappelli, C.; Corni, S.; Frediani, L.; Trucks, G. W.; Frisch, M. J. *Theor. Chem. Acc.* **2004**, *111*, 66−77.

(24) Islam, S. M. Poirier, R. A. *J. Phys. Chem. A*, in press, ASAP article on the web.

(25) Modro, A.; Schmid, G. H.; Yates, K. *J. Org. Chem.* **1977**, *42*, 3673−3676.

(26) Dubois, J. E.; Mouvier, G. *Bull. Soc. Chim. Fr*. **1968**, 1426−1435.

(27) Lenoir, D.; Chiappe, C. *Chem.*−*Eur. J*. **2003**, *9*, 1036−1044.

(28) Chiappe, C.; Rubertis, A. D.; Lemmen, P.; Lenoir, D. *J. Org. Chem*. **2000**, *65*, 1273−1279.

(29) Bellucci, G.; Bianchini, R.; Chiappe, C.; Ambrosetti, R.; Catalano, D.; Bennet, A. J.; Slebocka-Tilk, H.; Aarts, G. H. M.; Brown, R. S. *J. Org. Chem*. **1993**, *58*, 3401−3406.

(30) Brown, R. S. *Acc. Chem. Res.* **1997**, *30*, 131−137.

(31) Bellucci, G.; Bianchini, R.; Chiappe, C.; Marioni, F.; Ambrosetti, R.; Brown, R. S.; Slebocka-Tilk, H. *J. Am. Chem. Soc.* **1989**, *111*, 2640−2647.

(32) Frisch, M. J.; Trucks, G. W.; Schlegel, H. B.; Scuseria, G. E.; Robb, M. A.; Cheeseman, J. R.; Montgomery, J. A., Jr.; Vreven, T.; Kudin, K. N.; Burant, J. C.; Millam, J. M.; Iyengar, S. S.; Tomasi, J.; Barone, V.; Mennucci, B.; Cossi, M.; Scalmani, G.; Rega, N.; Petersson, G. A.; Nakatsuji, H.; Hada, M.; Ehara, M.; Toyota, K.; Fukuda, R.; Hasegawa, J.; Ishida, M.; Nakajima, T.; Honda, Y.; Kitao, O.; Nakai, H.; Klene, M.; Li, X.; Knox, J. E.; Hratchian, H. P.; Cross, J. B.; Bakken, V.; Adamo, C.; Jaramillo, J.; Gomperts, R.; Stratmann, R. E.; Yazyev, O.; Austin, A. J.; Cammi, R.; Pomelli, C.; Ochterski, J. W.; Ayala, P. Y.; Morokuma, K.; Voth, G. A.; Salvador, P.; Dannenberg, J. J.; Zakrzewski, V. G.; Dapprich, S.; Daniels, A. D.; Strain, M. C.; Farkas, O.; Malick, D. K.; Rabuck, A. D.; Raghavachari, K.; Foresman, J. B.; Ortiz, J. V.; Cui, Q.; Baboul, A. G.; Clifford, S.; Cioslowski, J.; Stefanov, B. B.; Liu, G.; Liashenko, A.; Piskorz, P.; Komaromi, I.; Martin, R. L.; Fox, D. J.; Keith, T.; Al-Laham, M. A.; Peng, C. Y.; Nanayakkara, A.; Challacombe, M.; Gill, P. M. W.; Johnson, B.; Chen, W.; Wong, M. W.; Gonzalez, C.; Pople, J. A. *Gaussian 03*, revision B.05; Gaussian, Inc.: Pittsburgh, PA, 2004.